

Document downloaded from:

<http://hdl.handle.net/10251/152257>

This paper must be cited as:

Teberio, F.; Arregui, I.; Soto Pacheco, P.; Laso, MA.; Boria Esbert, VE.; Guglielmi, M. (2017). High-Performance Compact Diplexers for Ku/K-Band Satellite Applications. IEEE Transactions on Microwave Theory and Techniques. 65(10):3866-3876.  
<https://doi.org/10.1109/TMTT.2017.2691773>



The final publication is available at

<https://doi.org/10.1109/TMTT.2017.2691773>

Copyright Institute of Electrical and Electronics Engineers

Additional Information

# High-Performance Compact Diplexer for Satellite Applications with Relaxed Fabrication Tolerances

Fernando Teberio, Ivan Arregui, Pablo Soto,  
Miguel A. G. Laso, Vicente E. Boria, and Marco Guglielmi

**Abstract**— In this paper, a very compact high-performance diplexer for satellite applications is presented. The diplexer has an overall bandwidth up to 50 %, and is composed of two novel band-pass filters (around 20 % and 7 % of relative bandwidth each one) joined together with an E-plane T-junction. The novel band-pass filters are designed by combining a low-pass filtering function (based on  $\lambda/4$ -step-shaped bandstop elements separated by very short waveguide sections) and a high-pass filtering structure (based on the waveguide propagation cutoff effect). The transmission band-pass filter provides the suppression of the higher-order modes over the reception band. The novel diplexer shows a very compact footprint and benefits of relaxed manufacturing tolerances. Moreover, it also achieves a very wide stopband for the reception channel and high-power operation. The final diplexer has been fabricated by milling, and the measurements of the device show a very good agreement with simulations, demonstrating the validity and manufacturing robustness of the proposed topology for stringent specifications.

**Index Terms**— Band-pass filter, low-pass filter, diplexer, tolerance analysis, waveguide filters.

## I. INTRODUCTION

COMMUNICATION satellite hardware requirements have become extremely stringent and demands high power, compact, low-weight, and low-cost products [1]-[3]. Furthermore, quick design and reduced manufacturing times are very important to obtain competitive products. The state-of-the-art of 3D-electromagnetic simulation tools and the accuracy of computer-controlled milling (CCM) machines offer great advantages in terms of production time and high-quality products. In order to obtain more economic devices, design times must be decreased, and manufacturing tolerances must be relaxed while maintaining a high production yield. Therefore, the development of design strategies that provide filters and diplexers less sensitive to fabrication techniques and their associated tolerances is in the spotlight.

This paper is an extended paper from the IEEE MTT-S International Microwave Symposium, May 22-27, 2016, San Francisco, CA.

This work was supported by the Spanish Ministry of Economy and Competitiveness under Projects TEC2014-55735-C3-R and TEC2013-47037-C5-1-R.

F. Teberio, I. Arregui, A. Gomez-Torrent, and M. A. G. Laso are with the Electrical and Electronic Engineering Department, Public University of Navarre, Pamplona 31006, Spain (e-mail: [fernando.teberio@unavarra.es](mailto:fernando.teberio@unavarra.es)).

M. Guglielmi, P. Soto, and V. E. Boria are with iTEAM – Dpto. de Comunicaciones, Universitat Politècnica de València, Valencia 46022, Spain.

The RF feed chain of communication satellites uses architectures with high-performance diplexers (overall bandwidths much larger than 20 % and operation passbands larger than 5 %) to separate the transmission and reception bands and combine them in a common antenna [4]-[6]. There are many diplexers in the technical literature which are based on classical bandpass filters with either inductive or capacitive couplings [7]-[8], or metal inserts [9]-[10]. If the relative bandwidth of the transmission or reception band is large, the use of this kind of filtering structures is not recommended. These scenarios normally require high order filters, and therefore compact size and low insertion loss cannot be achieved (in particular for the transmission band). Moreover, if the overall bandwidth of the diplexer extends in a very wide frequency range, higher-order modes could appear in the reception band. In such cases, the suppression of these higher-order modes is an important requirement that cannot be accomplished with the aforementioned filters. This issue can be solved in the transmission band with evanescent-mode filters [11], classical waffle-iron filters [12], or corrugated filters with a width reduction which shifts up in frequency the higher-order modes [13]. Lately, a high-power compact low-pass filter based on quarter-wave step-shaped bandstop elements separated by very short (ideally zero-length) waveguide sections has been proposed [14]. The performance of this novel structure has been compared with its classical counterparts in a high-performance diplexer showing that the size of the low-pass filter is dramatically reduced [6].

The aforementioned high-performance diplexer [6] uses, in the reception band, a classical inductive-iris filter designed with an optimum position of the couplings between the cavities to reduce the layout of the final diplexer. However, filters based on resonant cavities are more sensitive to manufacturing tolerances [15]. Some ideas to reduce the influence of the fabrication tolerances in classical coupled resonant structures (inductive and capacitive iris devices) such as the most obvious one, i.e. designing the filters to have sufficient margin to fulfill the frequency specifications at the cost of increasing the filter length, have been proposed in the literature [16]. In [17], the length of the resonating structures was enlarged to improve the tolerance issues. However, the latter implies that the overall size of the filter (and consequently the diplexer) increases as well and, besides, spurious resonances could appear below the passbands, which does not occur for half-wavelength resonators [18]. None of

this happens in the novel band-pass filters proposed in this paper, where relaxed fabrication tolerances and a compact size can be achieved simultaneously. Furthermore, waveguide band-pass filters based on either inductive or capacitive couplings [12], evanescent mode [11], and E-plane inserts [10] are susceptible to show spurious responses in the upper stopband, specifically due to undesired resonances or the propagation of higher-order modes. This does not happen with the topology proposed on this paper, due to the inherent non-resonating low-pass behavior of the band-pass structures included in the diplexer.

In this paper, two novel waveguide band-pass filters, susceptible to be fabricated using relaxed fabrication tolerances, are utilized to meet the Ku-band transmission (Tx) and reception (Rx) band specifications of a very compact high-performance diplexer with very stringent specifications for satellite applications. The aforementioned novel band-pass filters are designed by combining a low-pass waveguide filtering function following the technique described in [6], and a high-pass filtering function based on the cut-off effect [20] (Section II). Unlike [20], where both the height and length of the corrugations are design parameters, the design variables are only the height of the bandstop elements (since the required return loss is achieved with the matching networks,

which are also necessary to match the input/output block filter to the standard waveguide port dimensions). In fact, the proposed technique does not need large transformer elements (very short matching networks are used, as reported in [6]) thus leading to very compact devices.

The diplexer uses an E-plane T junction in L configuration to connect the filters (Section III). In comparison with the previous work [6], the total footprint has been dramatically reduced (around 40%), and the sensitivity to manufacturing tolerances has been significantly reduced. A prototype of the novel diplexer has been fabricated by CCM in aluminum, and the measured frequency response is very close to the simulation results (Section IV). Finally, the high-power behavior of the proposed diplexer including the novel band-pass filters has been analyzed using SPARK3D (Section V).

## II. NOVEL BAND-PASS FILTER DESIGN PROCEDURE

The in-band frequency response of the novel band-pass filters proposed in this paper is not based on coupled resonant structures as it happens in [17], [18] or in transmission lines of different characteristic impedances as it occurs in [20]. Instead, the passband characteristic has been realized by combining a reduced loss low-pass waveguide filter designed following the technique described in [6] and a high-pass configuration based on the cut-off effect [20]. The design procedure can be summarized in two steps: i) estimation of the required width and total length of the high-pass section, and ii) design the band-pass filter utilizing the low-pass filter function with the previous calculated parameters.

### A. High-Pass Filter Function

As it is well known, a rectangular waveguide can be seen as a high-pass filter where energy propagates only above the fundamental TE<sub>10</sub>-mode cutoff frequency [20].

The fundamental TE<sub>10</sub>-mode cutoff frequency of the high-pass filter function,  $f'$ , depends only on the dimensions of the waveguide and, specifically, on the width of the waveguide, and it should be chosen below the lower passband edge,  $f_l$ , of the bandpass filter. Therefore, the width of the high-pass filter function,  $a'$ , will be fixed according to (1):

$$a' = \frac{c}{2f'} \quad (1)$$

The attenuation of the travelling waves below cutoff grows exponentially along the filter length in the propagation direction ( $z$ -axis), following  $e^{-\alpha L_z}$ , where  $L_z$  is the length of the waveguide section and  $\alpha$  is the attenuation constant, which depends on the cutoff frequency as well as the width of the filter following (2):

$$\alpha = \frac{\pi}{a'} \sqrt{1 - \left(\frac{f'}{f_l}\right)^2} \quad (2)$$

Therefore, we will choose  $f'$  low enough to fulfil the required in-band return loss specifications of the lower passband edge,  $f_l$ , and to obtain a compact structure fulfilling

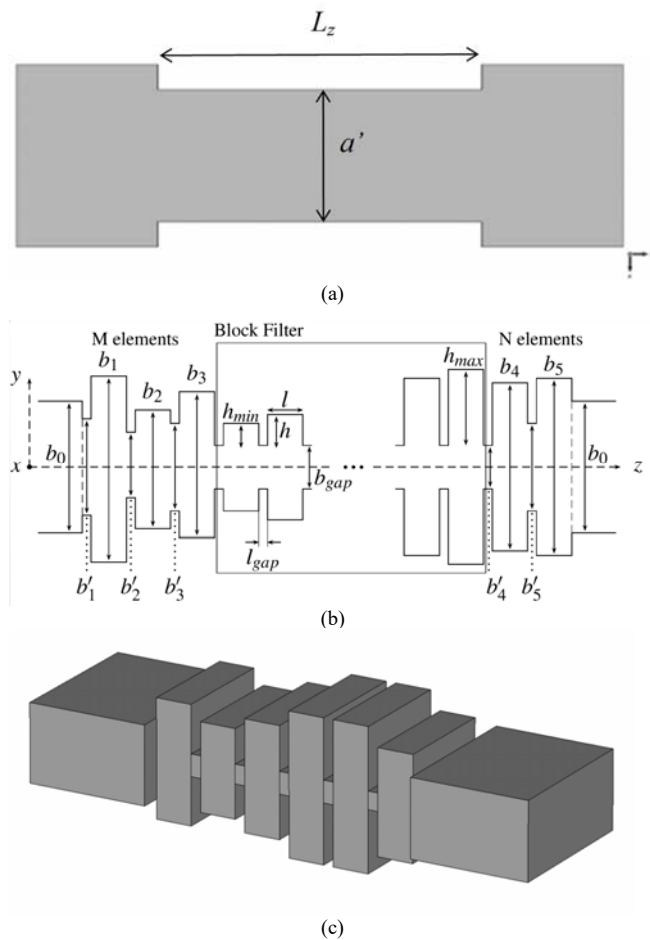


Fig. 1. Sketch of a novel band-pass filter with a constant high-pass width-reduction. (a) Top view (b) Side view, and (c) 3D view.

the required attenuation of the lower stopband (LSB) of the filter ( $Att_1$ ) following (3):

$$Att_1 = 20 \log(e^{\alpha L_z}) \quad (\text{dB}) \quad (3)$$

Finally, the constant and simple-to-fabricate width reduction (as can be seen Fig. 1(a)) can be utilized in the design of the band-pass filter to accomplish very steep cutoff characteristics near the cutoff frequency. The previous equations provide us with the value of the waveguide length of width  $a'$  that is necessary to obtain the required attenuation in the LSB,  $Att_1$ . Since this estimation is obtained assuming a straight waveguide section, and the device will present height variations, shorter lengths will be actually required. In fact, a much shorter length may be used if large modifications of the height are performed along the propagation direction, such as in this work. Therefore,  $L_z$  will determine the maximum length of the reduced width section which is required in the low-pass filter function designed in Subsection II.B.

### B. Low-Pass Filter Function

In [6], the possibility of achieving low-pass filtering structures for the suppression of the fundamental mode over a very wide stopband was demonstrated, and this technique will be applied, in combination with the theory described in Subsection II.A, to the design of the band-pass filter proposed in this paper. The attenuation of the upper stopband (USB) of the filter is achieved by means of  $n_{MB}$   $\lambda_g/4$ -step-shaped bandstop elements of different heights,  $h$ . The attenuation of the minimum frequency ( $f_{min}$ ) of the USB is achieved by means of the highest bandstop element ( $h_{max}$ ), and the maximum frequency of the upper stopband ( $f_{max}$ ) will be achieved with the shortest bandstop elements ( $h_{min}$ ). The length of the bandstop elements,  $l$  and the length of the waveguide sections between them,  $l_{gap}$ , as well as the minimum mechanical gap of the structure  $b_{gap}$ , are free parameters and can be fixed to obtain the desired high-power performance of the filter [21]. The width of the bandstop and the waveguide sections between them will be determined by the high-pass filtering function calculated in Subsection II.A. Finally, two matching networks are added to the input and output ports of the filtering structure to accomplish the intended in-band return loss of the filter (see Fig. 1 and [19] for more details).

## III. DIPLEXER: DESIGN CONSIDERATIONS

The specifications used in this paper to design the high-performance diplexer will be the same ones as those in [6] (detailed in Table I) with an additional attenuation in the Rx channel to signals between 27.5 and 31.5 GHz. The overall bandwidth of the diplexer is 53.4 %, and the fractional bandwidths are 19.4 % and 7.3 % for the transmission and reception band, respectively. In the diplexer design, the filters and the junction are designed independently, and then put together to obtain the final diplexer configuration.

### A. Requirements and Proposed Solution

A novel band-pass filter designed following the

forementioned design technique will be used to fulfil the Ku-band Tx specifications. The proposed filter achieves the suppression of the higher-order modes which could appear in the intended Rx band in a very compact size.

To cover the Ku-band Rx specifications, a band-pass filter following the same design technique, described in Section II, will be utilized, since it makes the design of the final diplexer less sensitive to manufacturing tolerances.

Lastly, once both filters are designed fulfilling the specifications, they are connected to an E-plane T-junction. The main advantage of the final diplexer configuration in comparison with [6] will be the dramatic footprint reduction.

### B. Band-Pass Filter for the Tx band

In [6], a more compact alternative to the classical waffle-iron filter or the corrugated filter with width modification was proposed. In this paper, a band-pass filter following the technique presented in Section II has also been designed.  $f_{TX}$  is set to 10 GHz, low enough to fulfill the intended in-band return loss specifications of the lower pass-band edge,  $f_{i,TX}$  (which is equal to 10.7 GHz), and to avoid the higher-order

TABLE I. SUMMARY OF DIPLEXER SPECIFICATIONS

Tx-band filter ( $f_{i,TX} - f_{2,TX}$ )	10.7 – 13 GHz
Rx-band filter ( $f_{i,RX} - f_{2,RX}$ )	17.2 – 18.5 GHz
Return loss at interface ports	> 20 dB
Insertion loss at interface ports	< 0.2 dB
Attenuation at Tx band ( $Att_{1,TX}$ )	> 50 dB
Attenuation at Rx band ( $Att_{2,RX}$ )	> 80 dB
Ku Tx-band interface port	WR75
Ku Rx-band interface port	WR51
Common interface port	WR75
Multipactor threshold level	> 2.5 kW

TABLE II. FINAL DIMENSIONS OF THE TX-BAND FILTER (mm)

Matching Networks	$M = 1$ element		$N = 1$ element	
		$h_{min}$	5.6	$h_{max}$
Main Block	$b_{gmin}$	3	$b_{gmax}$	3
	$l$	3	$l_{gap}$	0.825
High-Pass	$a'$	15	$L_z$	19.125

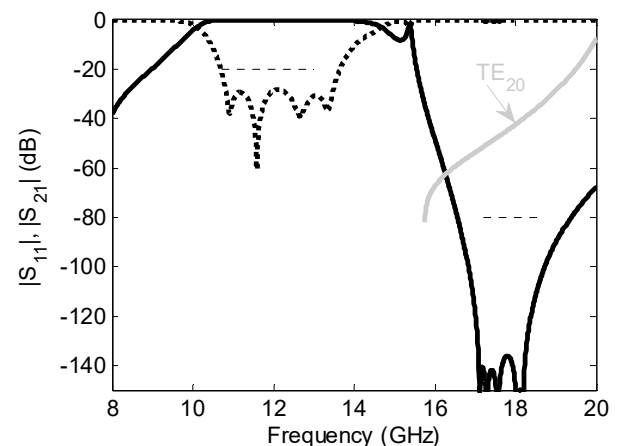


Fig. 2. FDTD simulated S-parameters ( $|S_{11}|$  in dotted line and  $|S_{21}|$  in solid line) for the TE<sub>10</sub> mode in the proposed Ku band Tx band-pass filter (black line) and for the higher-order modes (grey line) (rest of higher-order modes not shown are kept below -150 dB). Frequency specifications in dashed line.

TABLE III FINAL DIMENSIONS OF THE RX-BAND FILTER (mm)

Matching Networks	M = 1 element		N = 1element	
	$h_{min}$	4.24	$h_{max}$	4.26
Main Block	$b_{gmin}$	2	$b_{gmax}$	2
	$l$	4	$l_{gap}$	0.825
High-Pass	$a'$	9.375	$L_z$	19.3

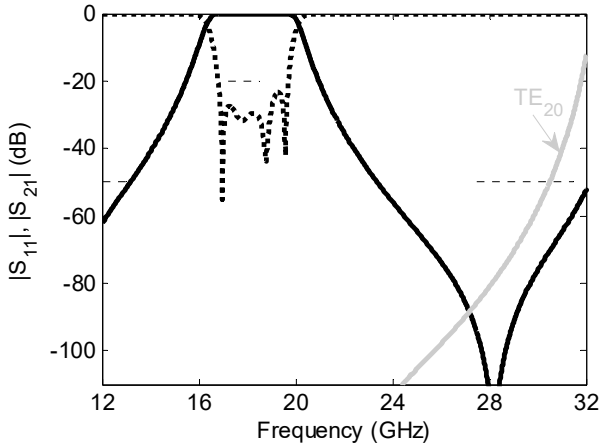


Fig. 3. FEST3D simulated S-parameters ( $|S_{11}|$  in dotted line and  $|S_{21}|$  in solid line) for the  $TE_{10}$  mode in the proposed Ku-Rx band-pass filter (black line) and for the higher-order modes (grey line) (rest of higher-order modes not shown are kept below -150 dB). Frequency specifications in dashed line.

$TE_{20}$  mode propagation over the Rx-band. The reduced width of the structure has been therefore fixed to 15 mm, which achieves both features. Since we do not have specifications for the LSB in this filter, the length of the width reduction along the propagation direction, which achieves the high-pass filtering function, does not have to be fixed to a specific value. The required attenuation of the USB of the filter ( $Att_{2,RX}$ ), is achieved by means of three  $\lambda_g/4$ -step-shaped bandstop elements, and the return loss of the filter is accomplished with only two elements, one at the input and one at the output of the block filtering structure (i.e., ultra-compact matching networks). The minimum mechanical gap of the structure,  $b_{gap}$ , has been fixed to 3 mm to achieve a high-power handling capability and the suppression of the higher-order non- $TE_{n0}$  modes ( $TE_{01}$ ,  $TE_{11}$ , and  $TM_{11}$ ). The physical dimensions of the final band-pass filter are detailed in Table II. The FEST3D simulated frequency response is depicted in Fig. 2. The filter shows an attenuation level better than 80 dB over the Rx-band and return loss better than 20 dB in the Tx-band. Moreover, the insertion loss of the filter is kept below 0.2 dB and the power threshold is better than 2.5 kW, as it will be shown in Section V. Also, the filter achieves the suppression of all higher-order modes up to 18.5 GHz.

### C. Band-Pass Filter for the Rx-band

A very-compact band-pass filter has been designed following again the technique proposed in Section II.  $f_{1,RX}$ , is equal to 17.2 GHz, and the required attenuation ( $Att_{1,TX}$ ) over the Tx band is equal to 50 dB (see Table I). Hence, if we choose  $f'$  equal to 16 GHz, the reduced width,  $a'$ , will be equal to 9.375 mm, the attenuation constant  $\alpha$  will be  $0.123 \text{ mm}^{-1}$  and the required length  $L_z$  for the high-pass filtering function

will be around 46.8 mm (using eqns. (1), (2), and (3)). As it has been explained previously, the  $L_z$ -length value is a first-order approximation of the final length in the reduced width section of the Rx filter. The required length of our filter will be even shorter due to the different heights of the structure.

The quarter-wave step-shaped bandstop elements are fixed to accomplish the required additional attenuation in the Rx channel to signals between 27.5 and 31.5 GHz, and only two elements, one at the input and one at the output port of the block filter are utilized to achieve the required return loss of the filter (as in the Tx-band filter, ultra-compact matching networks are possible). The final physical dimensions of the filter are detailed in Table III.

The frequency performance of the final filter is shown in Fig. 3. The insertion loss of the filter is kept below 0.2 dB and the multipactor threshold level is higher than 2.5 kW, as it will be shown in Section V. Furthermore, the Rx band-pass filter achieves the suppression of the higher-order modes up to 31.5 GHz (while the classical inductive-iris filter proposed in [6] does not achieve it).

### D. Junction and Common Port Interface

An E-plane T-junction has been chosen, although other different branching solutions could have been also used, e.g. bifurcations, manifolds, Y-junctions or H-plane T-junctions. An E-plane T-junction is a simple solution which allows fabricating the final device in clam-shell configuration, which will minimize the measured insertion loss of the prototype and the PIM products. The size of each port of the T-junction is  $5 \times 15$  mm. These dimensions ensure single-mode operation in the junction. In this paper, a height and width transformer has been utilized to achieve the size of the standard common port, since it leads to less spurious resonances in the final diplexer frequency response in comparison with the matching network that was used in [6].

## IV. DESIGN EXAMPLE: HIGH-PERFORMANCE COMPACT DIPLEXER

Once both filters are designed fulfilling the frequency specifications, they are connected together with the E-plane T-junction. Filters are joined directly to the junction by a waveguide section of minimum mechanical gap, since it minimizes the effect of spurious resonances between filters. The width and height of the common port are accomplished by means of a waveguide transformer with three sections.

Recently, a very interesting systematic method to design manifold-coupled multiplexers for wideband applications has been proposed in [22]. In the design of the diplexer of this paper, an analogous stepwise optimization procedure has been performed to obtain the final frequency response of the diplexer. Firstly, the length of each port of the E-plane T-junction are optimized. Then, we add to the optimization procedure the dimensions of the transformers and the short waveguide sections which connect each filter to the junction. After that, we add the dimensions of the first elements of each filter and, when the frequency response of the diplexer is very close to the required performance, all dimensions of the

diplexer are finely optimized. The optimization has been performed using the FEST3D optimizer module.

The final diplexer configuration can be seen in Fig. 4, showing a footprint of 34 x 42 mm, much more compact than the diplexer in [6] (45 x 65 mm). Specifically, a 50 % footprint reduction is achieved with regard to [8]. This is a

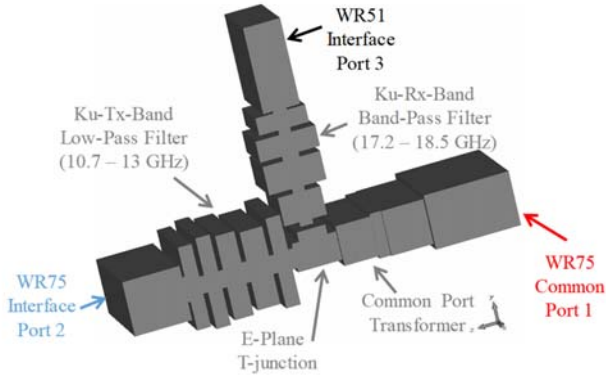


Fig. 4. 3D view of the diplexer configuration

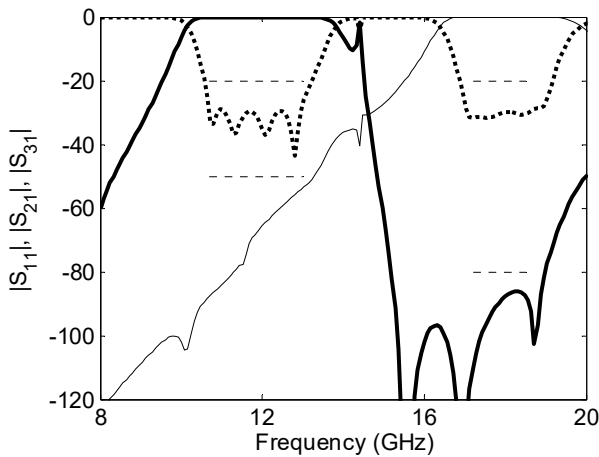


Fig. 5. FEST3D simulated frequency response of the novel compact high-performance diplexer.  $|S_{11}|$  in dotted line,  $|S_{21}|$  in solid thick line, and  $|S_{31}|$  in solid thin line. Frequency specifications in dashed line.

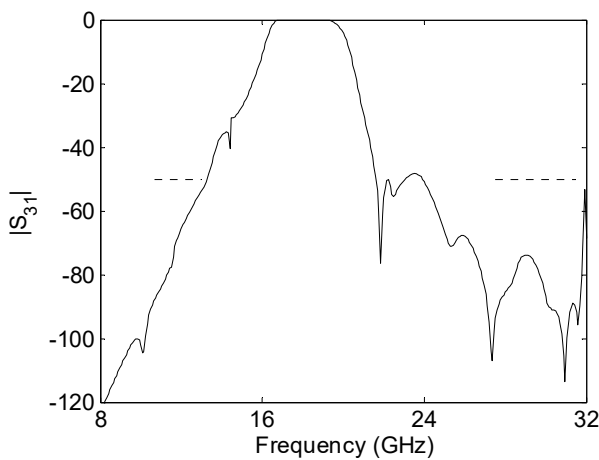


Fig. 6. FEST3D simulated  $|S_{31}|$  parameter of the novel compact high-performance diplexer showing the additional 50 dB attenuation in the Rx channel to signals between 27.5 and 31.5 GHz. Frequency specifications in dashed line.

great advantage in terms of mass and volume for satellite applications.

#### A. Simulation

The FEST3D simulated frequency response is presented in Fig. 5. The in-band return loss over the transmission band is better than 20 dB, and the attenuation level over the reception band is kept below 80 dB. Moreover, the return loss over the reception band also fulfils the frequency specifications. Furthermore, the rejection over the transmission band is better than 50 dB. Also, a 50 dB attenuation in the Rx channel to signals between 27.5 and 31.5 GHz is accomplished (see Fig. 6).

#### B. Sensitivity Analysis

A sensitivity analysis to manufacturing tolerances has been performed to demonstrate the robustness of the prototype. One hundred simulations varying all dimensions of the waveguide sections which compose the whole diplexer (heights, lengths,

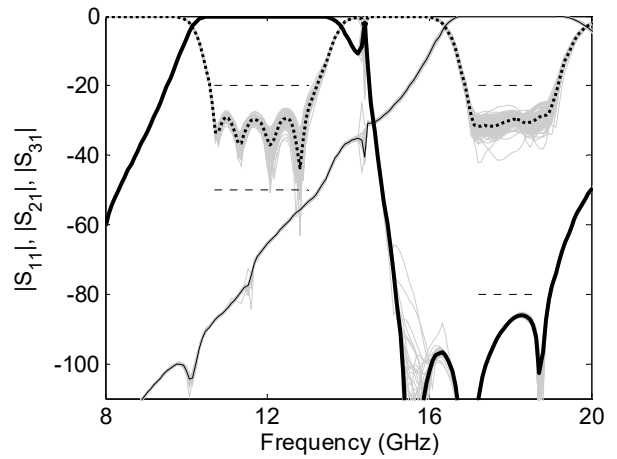


Fig. 7. Sensitivity analysis to fabrication tolerances ( $\pm 25$  microns) in the entire frequency response of the novel compact high-performance diplexer varying the physical dimensions of the filter.  $|S_{11}|$  in dotted line,  $|S_{21}|$  in solid thick line, and  $|S_{31}|$  in solid thin black line for the baseline filter. Grey lines: simulation trials. Frequency specifications in dashed line.

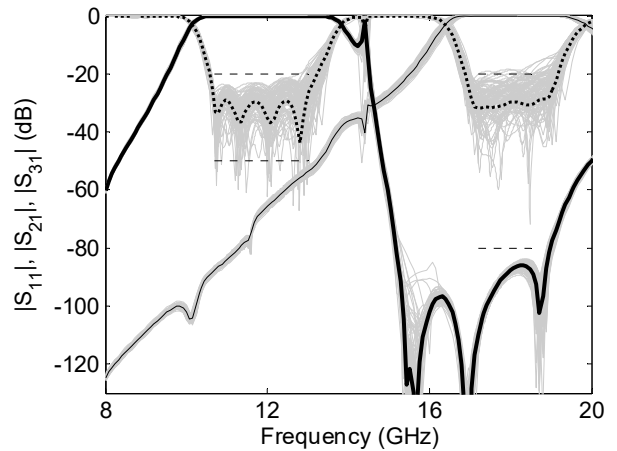


Fig. 8. Sensitivity analysis to fabrication tolerances ( $\pm 100$  microns) in the entire frequency response of the novel compact high-performance diplexer varying the physical dimensions of the filter.  $|S_{11}|$  in dotted line,  $|S_{21}|$  in solid thick line, and  $|S_{31}|$  in solid thin black line for the baseline filter. Grey lines: simulation trials. Frequency specifications in dashed line.

and widths) have been performed using FEST3D. The different physical dimensions are randomly generated by a Gaussian probability density function with a standard deviation equal to 0,01 mm. This function corresponds, approximately, to a worst-case error value of  $\pm 25$  microns (i.e., low-cost CCM manufacturing tolerances). As can be seen in Fig. 7, curves show an excellent fitting to the ideal frequency response. In fact, the predicted manufacturing yield is 100 %.

Moreover, a full sensitivity analysis has been performed taking into account a Gaussian probability density function with a standard deviation equal to 0,04 mm; in order to foresee future issues if we wanted to fabricate the proposed diplexer with low-cost 3-D printers. This function corresponds, approximately to a worst-case error value of  $\pm 100$  microns. As it is shown in Fig. 8, most of the cases fulfil the frequency specifications, showing a predicted manufacturing yield of 85 %.

Therefore, both previous analyses demonstrate the low sensitivity to manufacturing tolerances of the very compact high-performance diplexer, including two novel band-pass filters designed following the technique described in Section II. In conclusion, the diplexer could be easily produced by cheap 3-D printing technology, or by low-cost

CCM as reported in Subsection IV.C.

### C. Fabrication and Measurements

A prototype has been fabricated by CCM with aluminum in two identical halves in clam-shell configuration. For a low-cost manufacturing, it is necessary to take into account the rounding of the diplexer corners corresponding to classical milling techniques. Unlike [6], where the rounded corners must be considered in the optimization procedure (since classical inductive-coupled filters are very sensitive to rounded corners [23]), the rounding of the corners was not considered in the optimization procedure of the diplexer in this paper, since the filters proposed in this work are robust enough not to be affected by this issue. The final configuration of the diplexer taking into account rounded corners is shown in Fig. 9. As can be seen in Fig. 10, there are almost no relevant differences between the frequency response of the diplexer with sharp corners and rounded corners. This allows an easy and very quick design process, since taking rigorously into account rounded corners is a time-consuming task during the optimization.

The fabricated prototype is shown in Fig. 11. The diplexer has been measured using an Agilent E8364B PNA, proper waveguide-to-coaxial transitions, waveguide tapers, loads, and calibration kits. The measurements has been carried out in WR75 (10-15 GHz) and WR51 (15-20 GHz) bands. The

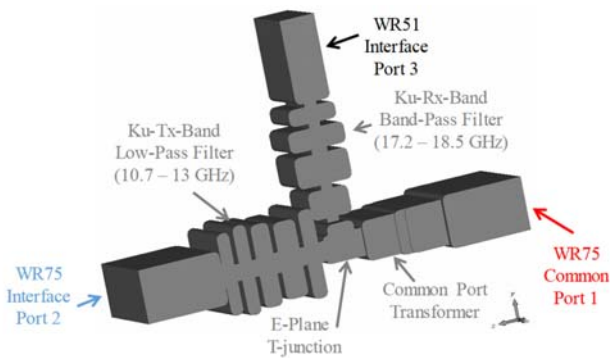


Fig. 9. 3D view of the diplexer configuration with rounded corners.

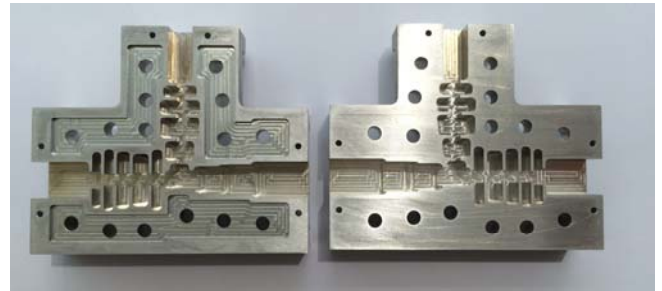


Fig. 11. Photograph of the unassembled prototype fabricated by computer-controlled milling in aluminum in clam-shell configuration.

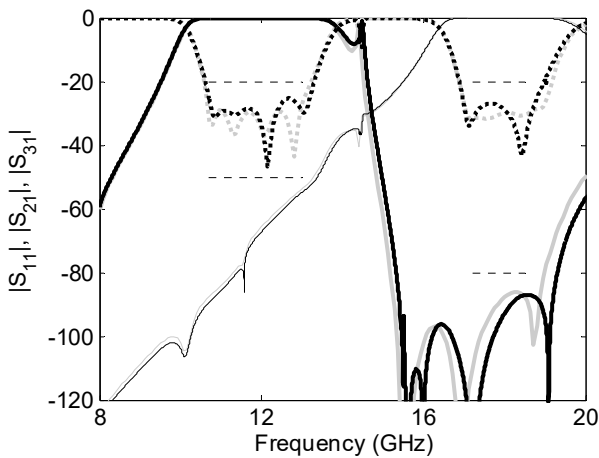


Fig. 10. Comparison between the simulated frequency response taking into account the rounding of the corners (CST MWS) on the proposed diplexer (black line), and without the rounded corners (FEST3D) (grey line).  $|S_{11}|$  in dotted line,  $|S_{21}|$  in solid thick line, and  $|S_{31}|$  in solid thin line. Frequency specifications in dashed line.

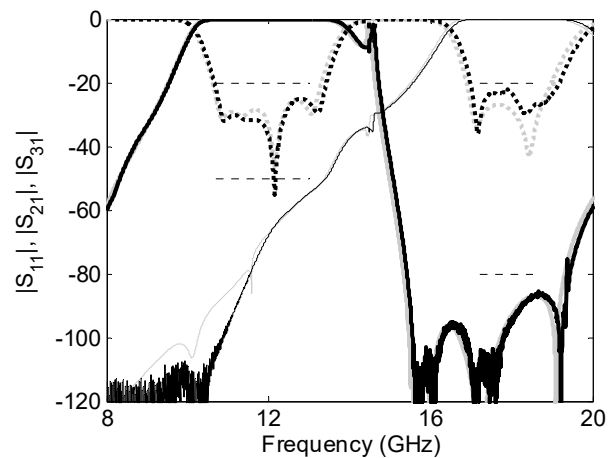


Fig. 12. Comparison between the CST MWS simulated frequency response (grey line) of the final diplexer with rounded corners and measurements of the fabricated prototype (black line).  $|S_{11}|$  in dotted line,  $|S_{21}|$  in solid thick line, and  $|S_{31}|$  in solid thin line. Frequency specifications in dashed line.

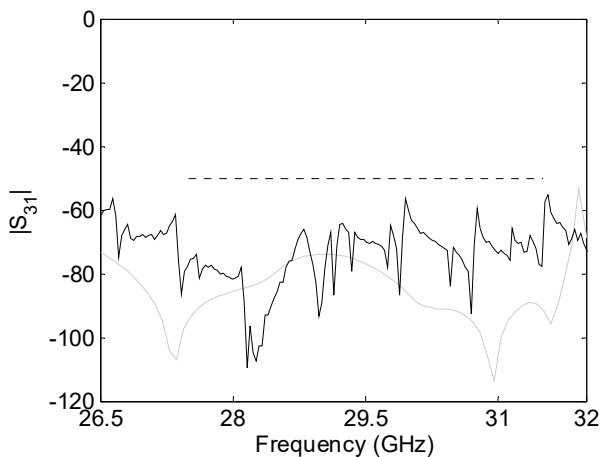


Fig. 13. Detail of the additional rejection in the 27.5 – 31.5 GHz in the Rx band. Comparison between the CST MWS simulated  $|S_{31}|$  parameter (grey line) of the final diplexer with rounded corners and measurements of the fabricated prototype (black line). Frequency specifications in dashed line.

TABLE IV. SUMMARY OF MULTIPACTOR THRESHOLD LEVELS OF THE NOVEL DIPLEXER AT DIFFERENT FREQUENCIES (SPARK3D)

10.7 GHz	13 GHz	17.2 GHz	18.5 GHz
> 40 kW	> 10 kW	> 80 kW	> 100 kW

measurements (see Fig. 12) show an attenuation level better than 80 dB in the Tx-band and better than 50 dB in the Rx-band. Moreover, the measured in-band return loss of the filter is kept better than 20 dB in both the Tx- and the Rx-band. The insertion loss of the diplexer is kept below 0.2 dB for each band.

Finally, the additional rejection in the Rx channel has been measured in WR28 (26.5-32 GHz). As can be seen in Fig. 13, the attenuation achieved for these frequencies is better than 50 dB, fulfilling also this goal.

#### V. HIGH-POWER ANALYSIS

The high-power behavior of the compact high-performance diplexer designed in Section IV has been estimated by means of SPARK3D, considering the electromagnetic fields previously calculated with CST MWS. The four passband frequencies edges have been utilized in the analysis (10.7 GHz, 13 GHz, 17.2 GHz, and 18.5 GHz), since these are the critical frequencies at which electromagnetic fields are maximum. The secondary emission yield (SEY) of aluminum has been used.

The worst case of multipactor threshold level has been obtained at 13 GHz (all results are summarized in Table IV). The novel compact high-performance diplexer can handle up to 10 kW. It is important to note that if the diplexer was silver-plated, the multipactor threshold level would be higher (since the SEY of silver is lower than the SEY of aluminum).

#### VI. CONCLUSION

In this paper, a very compact high-performance diplexer has been presented, including two novel band-pass filtering structures. The proposed band-pass filters are designed by

combining a low-pass and a high-pass response. The high-pass response is achieved by means of a width reduction along the propagation direction of the filter, making use of the waveguide cutoff effect. The low-pass response is based on quarter-wave step-shaped bandstop elements separated by very short waveguide sections, which achieve the low-pass attenuation of the filter. Two extremely short matching networks are added to accomplish the required return loss of the structure. This technique allows obtaining very compact filters with relaxed fabrication tolerances. Moreover, high-power behavior and very wide stopbands can be also accomplished. The novel diplexer shows an overall bandwidth up to 50 % and a very compact size (around 50 %-footprint reduction in comparison with [6]), which makes it especially attractive for satellite applications, where compact hardware is needed. A Ku-band prototype has been manufactured by milling in clam-shell configuration demonstrating the validity of the novel diplexer, confirmed with the very close agreement between simulations and measurements.

#### ACKNOWLEDGMENTS

The authors thank the European High RF Power Space Laboratory of European Space Agency (ESA) and Val Space Consortium (VSC) for contributing with its measuring installations – Laboratory co-funded by the European Regional Development Fund – A way of making Europe.

#### REFERENCES

- [1] D. Scouarnec, S. Stirland, and H. Wolf, "Current antenna products and future evolution trends for Telecommunication satellites application," in *Proc. 2013 IEEE-APS Topical Conference on Antennas and Propagation in Wireless Communications (APWC)*, pp. 1412-1415, Torino, Italy, Sept. 2013.
- [2] A. Abramowicz, A. Sibiga, and M. Znojkwicz, "Design and realization of low-cost waveguide filters and diplexers," in *Proc. 14th International Conference on Microwaves, Radar and Wireless Communications*, vol.2, pp.603-606, 2002.
- [3] J.R. Aitken and J. Hong, "Tolerance considerations for wireless backhaul diplexer circuits," in *Proc. 44th European Microwave Conference*, pp. 620-623, Rome, Italy, Oct. 2014.
- [4] J. Uher, J. Bornemann, and U. Rosenberg, *Waveguide Components for Antenna Feed Systems: Theory and CAD*. Artech House, 1993.
- [5] U. Rosenberg, A. Brandt, M. Perelshtein, and P. Bourbonnais, "Extreme broadband waveguide diplexer design for high performance antenna feed systems," in *Proc. 40th European Microwave Conference*, pp. 1249-1252, Paris, France, Sept. 2010.
- [6] F. Teberio, I. Arregui, M. Guglielmi, A. Gomez-Torrent, P. Soto, M.A.G. Laso, and V. Boria, "Compact Broadband Waveguide Diplexer for Satellite Applications," in *Proc. IEEE MTT-S*, San Francisco, CA, May 2016.
- [7] J. M. Rebolgar, J. R. Montejo-Garai, A. Ohoro, "Asymmetric H-plane T-junction for broadband diplexer applications," *IEEE APS-S*, vol. 4, pp. 2032-2035, Jul. 2000.
- [8] J. Bornemann, M. Mokhtaari, "The bifurcated E-plane T-junction and its application to waveguide diplexer design," in *Proc. German Microwave Conf.*, 1a-5, 4 p., Karlsruhe, Germany, Mar. 2006.
- [9] J. Dittloff, F. Arndt, "Computer-Aided Design of slit-coupled H-plane T-junction diplexers with E-plane metal-insert filters," *IEEE Trans. on Microw. Theory and Techn.*, vol. 36, no. 12, pp. 1833-1840, Dec. 1988.
- [10] E. Ofli, R. Vahldieck, and S. Amari, "Novel E-plane filters and diplexers with elliptic response for millimeter-wave applications," *IEEE Trans. on Microw. Theory and Techn.*, vol. 53, no. 3, pp. 843-851, Mar. 2005.

- [11] R. V. Snyder, "New application of evanescent mode wave-guide to filter design," *IEEE Trans. on Microw. Theory and Techn.*, vol. 25, no. 12, pp. 1013-1021, Dec. 1977.
- [12] G. L. Matthaei, L. Young, and E. M. T. Jones, *Microwave Filters, Impedance-Matching Networks, and Coupling Structures*. Norwood: Artech House, 1980.
- [13] W. Hauth, R. Keller, and U. Rosenberg, "CAD of waveguide low-pass filters for satellite applications," in *17th Eur. Microw. Conf.*, Rome, Italy, pp. 151-156, 7-11 Sept. 1987.
- [14] F. Teberio, I. Arregui, A. Gomez-Torrent, E. Menargues, I. Arnedo, M. Chudzik, M. Zedler, F. -J. Görtz, R. Jost, T. Lopetegui, and M. A. G. Laso, "High-power waveguide low-pass filter with all-higher-order mode suppression over a wide-band for Ka-band satellite applications," *IEEE Microw. Wireless Compon. Lett.*, vol. 25, no. 8, pp. 511-513, Aug. 2015.
- [15] J. Bornemann, U. Rosenberg, S. Amari, and R. Vahldieck, "Tolerance analysis of bypass-, cross-, and direct-coupled rectangular waveguide band-pass filters," *IET Microwaves, Antennas and Propagation*, vol. 152, no. 3, pp. 167-170, Jun. 2005.
- [16] A. Morini, G. Venanzoni, M. Farina, and T. Rozzi, "Practical design of a high-power tuning-less W-band triplexer for ground radar surveillance systems," *IET Microwaves, Antennas and Propagation*, vol. 1, no. 4, pp. 822-826, Aug. 2007.
- [17] J.R. Aitken and J. Hong, "Design of millimeter wave diplexers with relaxed fabrications tolerances," *IET Microwaves, Antennas and Propagation*, vol. 9, no. 8, pp. 802-807, 2015.
- [18] G. Cannone and M. Oldoni, "High-yield E-band diplexer for fixed radio point-to-point equipment," *International Journal of RF and Microwave Computer-Aided Engineering*, vol. 24, no. 4, pp. 508-512, Dec. 2013.
- [19] F. Teberio, I. Arregui, A. Gomez-Torrent, E. Menargues, I. Arnedo, M. Chudzik, M. Zedler, F. -J. Görtz, R. Jost, T. Lopetegui, and M. A. G. Laso, "Low-loss compact Ku-band waveguide low-pass filter," in *Proc. IEEE MTT-S*, Phoenix, May 2015.
- [20] W. Hauth, R. Keller, and U. Rosenberg, "The corrugated-waveguide band-pass filter – A new type of waveguide filter," in *Proc. 18th European Microwave Conference*, pp. 945-949, Stockholm, Sweden, Sept. 1988.
- [21] F. Teberio, I. Arregui, A. Gomez-Torrent, I. Arnedo, M. Chudzik, M. Zedler, F. -J. Görtz, R. Jost, T. Lopetegui, and M. A. G. Laso, "Chirping techniques to maximize the power-handling capability of harmonic waveguide low-pass filters," *IEEE Trans. on Microw. Theory and Techn.*, to be published.
- [22] C. Carceller, P. Soto, V. Boria, M. Guglielmi, and J. Gil, "Design of compact wideband manifold-coupled multiplexers," *IEEE Trans. on Microw. Theory and Techn.*, vol. 63, no. 10, pp. 3398-3407, Oct. 2015.
- [23] S. Cogollos, V. E. Boria, P. Soto, B. Gimeno, and M. Guglielmi, "Efficient CAD tool for inductively coupled rectangular waveguide with rounded corners," in *Proc. 31th European Microwave Conference*, pp. 1-4, London, England, Sept. 2001.